Review

Permeability: The Driving Force That Influences the Mechanical Behavior of Polymers Used for Hydrogen Storage and Delivery

Emanuele Sgambitterra and Leonardo Pagnotta *

Department of Mechanical, Energy and Management Engineering, University of Calabria, 87036 Rende, Italy; emanuele.sgambitterra@unical.it
* Correspondence: leonardo.pagnotta@unical.it

Abstract: This article explores the main mechanisms that can generate damage in polymers and polymer-based materials used for hydrogen storage and distribution infrastructures. All of these mechanisms are driven by the permeability process that is enhanced by the operating temperature and pressure conditions. Hydrogen storage and delivery systems typically work under high pressure and a relatively wide range of temperatures, especially during the filling and emptying processes. Therefore, it is of great interest to better understand how this phenomenon can influence the integrity of polymer-based hydrogen infrastructures in order to avoid catastrophic events and to better design/investigate new optimized solutions. The first part of this paper discusses the main storage and delivery solutions for gas and liquid hydrogen. Then, the physics of the permeability is investigated with a focus on the effect of pressure and temperature on the integrity of polymers working in a hydrogen environment. Finally, the main mechanisms that mostly induce damage in polymers operating in a hydrogen environment and that influence their mechanical properties are explored and discussed. Particular focus was placed on the rapid gas decompression and aging phenomena. In addition, some of the limits that still exist for a reliable design of polymer-based storage and delivery systems for hydrogen are pointed out.

Keywords: hydrogen; polymers; permeability; rapid gas decompression; aging

1. Introduction

Energy plays a fundamental role in our society and in our daily lives. Lighting systems, office machines, household appliances, and electronic devices work thanks to electricity. Transportation and, therefore, trade are made possible by petroleum products. Industry as well as agriculture depend on energy supply for their activities.

Energy resources are fundamentals for the development of international orders in modern history: coal was the backdrop to the British Empire in the 19th century; oil was at the heart of the "American century," and today, many people think that China would become the global renewable energy superpower of this century. In fact, in 2015, China had the largest financial commitment to renewable energy, investing over USD 100 billion. This represents a significant increase from over USD 3 billion a little over a decade ago [1]. In addition, as of recent data, China's renewable power capacity has reached a record high: hydropower [1], 420 million kW (including conventional hydropower and pumped storage hydropower); wind power, 404 million kW; solar power, 536 million kW; biomass power, 44 million kW23. In a few words, one can state that energy is strategically important, and it defines global economic and geopolitical dynamics.

Over the last twenty years, the global role of energy has become even more central as a consequence of two major issues, climate change and energy access, in developing countries.

Global energy supply has always been largely based on fossil fuels. Despite the recent development of renewable energy, 80% of the world's energy supply still comes from coal, oil, and natural gas (see Figure 1a), whose combustion produces around 75% of global

greenhouse gas emissions, making energy the main cause of climate change (see Figure 1b). A structural response to this serious worldwide problem can only come from the energy sector, in particular, through a global clean energy revolution.
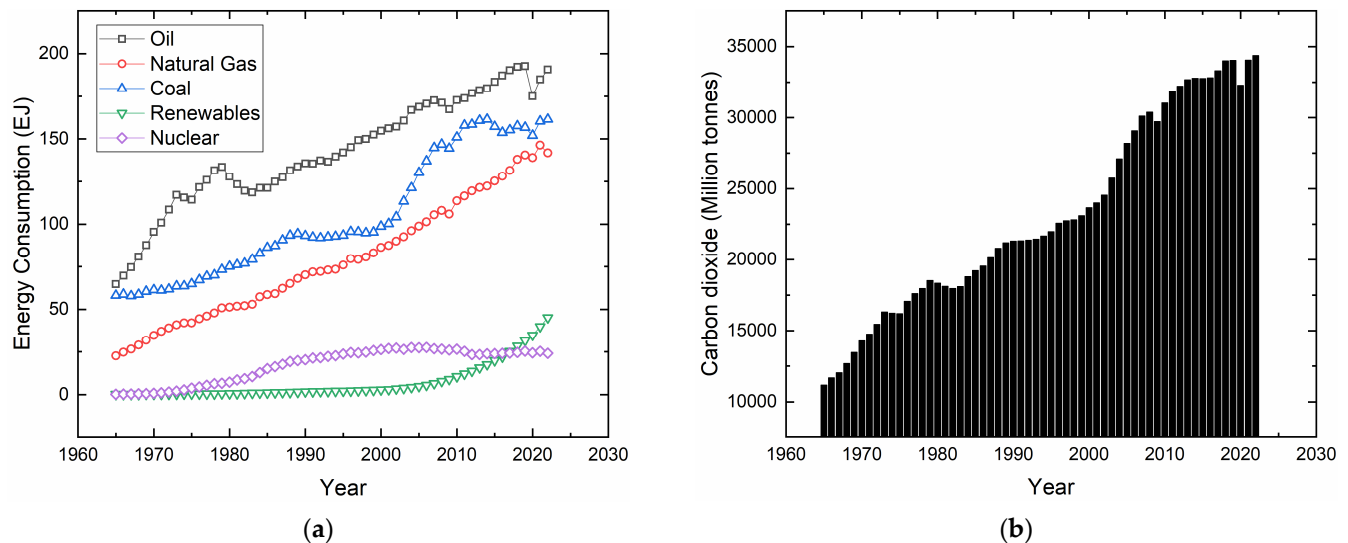
Figure 1. (**a**) Evolution of the energy consumption coming from oil, natural gas, coal, renewables, and nuclear energy sources. (**b**) Evolution of the generated carbon dioxide through consumption of oil, gas, and coal for combustion-related activities. Data are obtained from the Statistical Review of World Energy.

For this reason, in the last decades, many efforts have been devoted to developing new technologies for the most sustainable green energy production, such as wind turbines, solar panels, biomass, or hydropower systems. It is evident that renewable energy generation resources provide a more sustainable solution than fossil fuels [2,3]. In fact, they produce electricity with enhanced cost-effectiveness, increased efficiency, and superior environmental profiles [4,5]. Most studies revealed big improvements in terms of productivity and cost-benefit [5–7] in energy production, with relatively small effects on the environment [8,9]. However, it is important to underline that renewable power plants are also associated with emissions [10,11], mostly generated during the extraction and transportation of raw materials and the end-of-life waste management period [12]. In any case, these emissions are lower than the ones coming from conventional power-generating units but are not negligible [13].

In addition, the actual renewable energy sources are strongly weather-dependent, and this can generate a noncontinuous power supply if they are directly connected to an electric grid, and variability of the production. Storing the produced energy and providing it when the demand is high represents a keyword for an efficient energy supply. Unfortunately, the actual technologies are not properly feasible, and the storage capacity is quite limited. A possible solution is represented by the conversion into another form, as electrolysis accomplishes by transforming electricity into oxygen and hydrogen (H_2) [14]. The latter can be stored in different forms, converted into another gas, or, again, into electricity in a fuel cell [15].

Thanks to these properties, nowadays, hydrogen represents one of the most challenging and promising energy carriers and suppliers due to its high energy density, clean-burning characteristics, and sustainability [16], and it is quite evident that it will have a key role in the transition toward a sustainable and green society [17].

Hydrogen can be produced from renewable sources such as biomass, solar, wind, geothermal, as well as conventional non-renewable sources [18,19]. The production of hydrogen from renewable sources is gaining scientific attraction and can be achieved with

zero carbon emissions [20]. Hydrogen, as an energy carrier, has the potential to store energy locally and supply heat and electricity to buildings without emissions [21].

Nonetheless, in order to be efficient and competitive in everyday applications, hydrogen requires a robust and secure system. This system should ensure safety during processes such as delivery, storage, and end-use strategies [22]. The effectiveness of these procedures heavily relies on advancements in technology and suitable materials.

In this review, the state of the art of the actual storage and delivery system for hydrogen is discussed, and the main issues related to the used material are investigated. This work is focused on the polymeric materials that, nowadays, are the most reliable in hydrogen infrastructures. In fact, they are characterized by proper mechanical properties that make them the best solution. However, even polymers are susceptible to hydrogen exposure, especially as a consequence of the permeability process that triggers damage initiation and evolution.

This article explores these damage mechanisms by linking them to the permeability process. In addition, as permeability is pressure- and temperature-dependent, their influence on the integrity of polymer-based hydrogen infrastructures is analyzed.

2. Hydrogen: Main Properties

Hydrogen is the simplest element in nature, which consists of a nucleus made of a single proton and an electron orbiting around it. It is the lightest element, with a very low density: one can consider that in the gaseous state, at laboratory pressure and temperature, the density of hydrogen is only 0.0824 kg/m^3, whereas the air density under the same conditions is 1.184 kg/m^3. This means that large storage volumes are required. This property makes hydrogen advantageous for filling processes but disadvantageous when dealing with transportation and storage. It is a colorless, odorless, and non-toxic gas. It liquefies at ambient pressure and a temperature of -250 °C.

Compared with other fuels, hydrogen exhibits the largest amount of energy for the same mass (120 MJ/kg). When liquefied at a temperature of -250 °C, its density is only 70.79 g/m^3, resulting in an extremely low volumetric energy content, i.e., 0.01 MJ/L at the gas state and 8.5 MJ/L for the liquid one [23]. To give a better idea, the volumetric energy contents of methane and gasoline are 0.04 MJ/L and 32 MJ/L, respectively.

It is important to note that liquid hydrogen always requires special isolation systems for storage and transportation in tanks, and large quantities of energy are necessary to obtain it.

All these properties have a big influence on the design/selection of the storage and transportation systems. In addition, it is important to underline that hydrogen, according to the storage methodology, can have a strong impact on the mechanical performance of the material used [24]. All these aspects are explored in the following sections.

3. Hydrogen Embrittlement

As previously discussed, hydrogen transportation and storage represent a growing interest field within the scientific community, especially in view of the reduction in greenhouse gas emissions, which is a global goal. However, some technical aspects must necessarily be addressed as a consequence of the effect that hydrogen has on common metallic materials, such as hydrogen embrittlement (HE). The latter is an extremely important phenomenon to take into account, as it can lead to catastrophic failures in storage and transportation systems.

The mechanisms that drive HE can be distinguished in three different steps [25]:

1. Absorption of hydrogen within the material (see Figure 2). This phenomenon is sped up by increasing the temperature, and it can be hindered if the surface of the material is covered by an oxide layer. The latter, in fact, tends to reduce the degree of dissociation of H_2 molecules;

2. Diffusion of hydrogen through the metal lattice. During this process, atoms occupy interstitial sites, such as grain boundaries, vacancies, and other areas, with sufficient

volume to accommodate new hydrogen, remaining entrapped inside these material defects (see Figure 2);

3. Trapped hydrogen will generate localized stress concentration due to the volume mismatches of the microstructures, leading to crack propagation until the final failure of the component (see Figure 2).
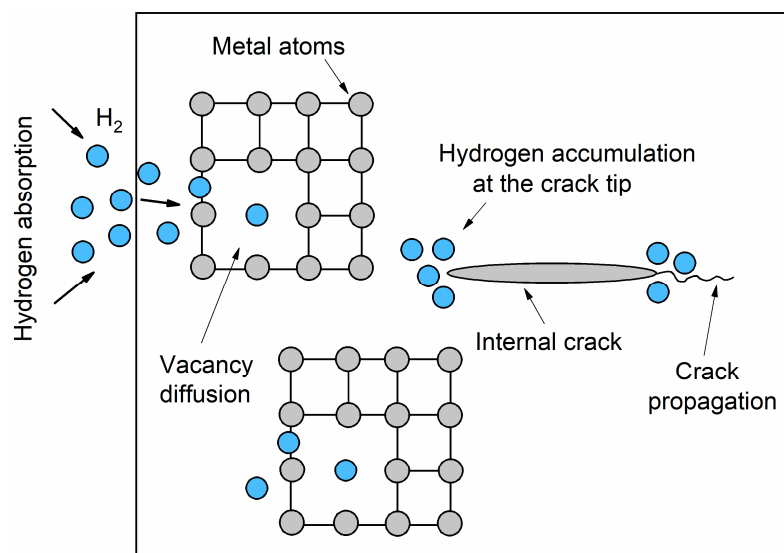
Figure 2. Schematic illustration of hydrogen atoms interacting with metal crystal lattice.

The main consequence of HE is the deterioration of the mechanical properties of the materials in terms of ductility and toughness. These effects are enhanced by both the temperature and the pressure. In particular, concerning the temperature, the reason has to be attributed to the speeding up diffusion mechanism according to Arrhenius' law (see Section 8). The influence of hydrogen gas pressure, instead, has to be attributed to the increasing amount of atomic hydrogen per unit of volume, which induces an increase in the crack propagation rate [26].

In the following two sections, the typical way to store and deliver hydrogen is discussed. The evolution of the employed materials aimed at reducing catastrophic events that could also be induced by HE is analyzed with the aim of understanding the reason why polymeric materials today represent the best technological solution.

4. Hydrogen Storage Vessels

Nowadays, there are different new trends in hydrogen storage technologies under investigation by the scientific community, such as solid-state hydrogen storage [27]. The latter includes metal hydrides [28], carbon-based materials, organic metal skeletons, and borohydride. Recently, liquid organic hydrogen carriers (LOHCs) technology has also shown great potential for efficient and stable hydrogen storage and transport [29].

However, the most common ways to store H_2 today are still gas compression, liquefaction, and cryo-compression [30–34].

Gas compression is the most common storage technology for both stationary and delivery applications; in fact, standards and regulations have been developed for different applications.

Pressure vessels are mostly used in the industrial field to store in situ and in mobility for the onboard power supply and storage in refueling stations. However, this solution still requires a deeper understanding of the materials and geometrical aspects in order to guarantee its safe application. Nowadays, safety also represents a crucial aspect because hydrogen faces increased public concern about hydrogen-related risks due to major accidents involving hydrogen, including the Hindenburg fire in 1937 and the hydrogen explosion in the Fukushima nuclear plant in 2011 [35].

Currently, compressed hydrogen can be stored in five different typologies of pressure vessels (named from Type I to Type V) that can be pressurized up to 70 MPa [30]:

1. Type I pressure vessels are the most conventional and the cheapest, but they are also quite heavy. In fact, they are typically made of metal alloys (steel or aluminum) and are mainly used for industrial applications with pressures ranging from 20 to 30 MPa (see Figure 3). However, for high hydrogen pressures or densities, the vessel wall needs to be relatively thick. These are also used in refueling stations;

2. Type II pressure vessels are made of metal (mostly steel or aluminum) wrapped with fiber resin composite to improve the structural resistance (see Figure 3). Compared to Type I, this type of vessel is lighter but is the most expensive for the manufacturing process;

3. Type III pressure vessels are made of carbon fiber composite materials embedded in a polymer matrix and a metallic inner liner (made of steel or aluminum) that is applied for sealing purposes (see Figure 3). They are reliable when used up to a pressure of 45 MPa; some studies also investigated higher pressure, up to 70 MPa, but at this level, they experienced some problems [36]. Compared to Type II, Type III pressure vessels are half the weight, but their cost is twice as high;

4. Type IV pressure vessels, as well as Type III, are entirely made of composite materials and an inner liner. However, compared to Type III, where the liner is mostly metallic, in Type IV, the liner is mostly polymeric as it is made of high-density polyethylene (HDPE) (see Figure 3). Type IV pressure vessels can withstand pressures up to 100 MPa;

5. Type V vessel is a modification of Type IV vessel with reinforcing space-filling skeletons [37] and is designed to contain hydrogen with even higher volumetric and gravimetric densities, see Figure 3. These vessels are, however, not yet available commercially. More detailed construction features of the hydrogen storage vessels are given by Barthelemy et al. [36].
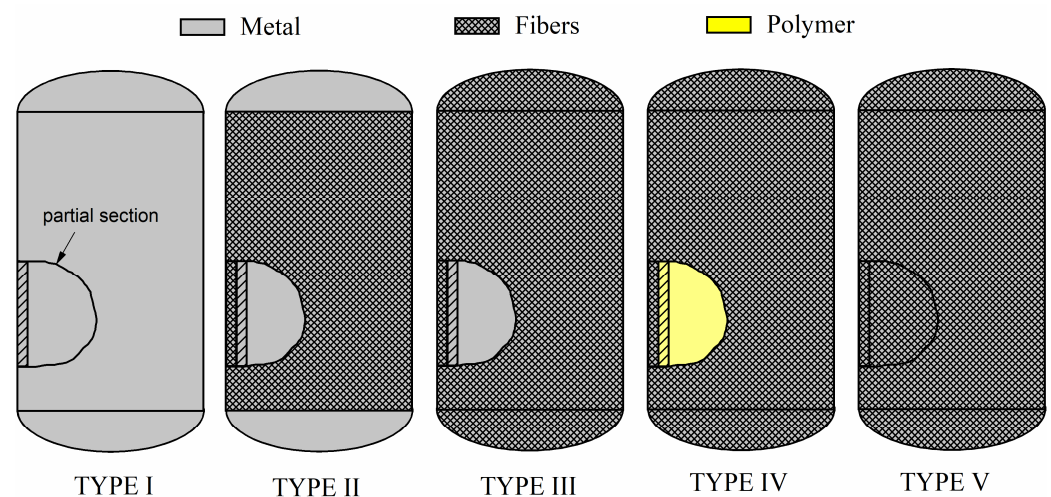
Figure 3. Schematic representation of the storage methods.

Liquid hydrogen can also be stored and transported in vessels. In this case, relatively low pressure (~0.6 MPa) can be used; however, as the operating temperatures are very low, below the critical point of the hydrogen ($-250\,^{\circ}$C), these vessels need very strict thermal insulation requirements. In this particular case, vessels consist of an inner metallic vessel surrounded by vacuum insulation to minimize evaporation losses and an outer metallic vacuum jacket [38]. They are usually cylindrical or spherical and typically have redundant pressure relief devices for safety conditions in order to prevent over-pressurization.

Cryo-compressed hydrogen represents a state where it exists as a supercritical cryogenic gas. Unlike liquefaction, which does not occur in this case, gaseous hydrogen is

compressed at approximately −233 °C. Cryo-compressed storage offers several advantages, including a high storage density (80 g/L, which is approximately 10 g/L higher than cryogenic storage), rapid and efficient refueling, and enhanced safety due to the presence of a vacuum enclosure. Cryo-compressed vessels are compatible with both high pressure (35 MPa) and cryogenic temperatures due to liquid hydrogen (−250 °C). They comprise a Type III aluminum-composite vessel surrounded by a vacuum space and an outer metallic vacuum jacket [39].

Comparing the different types of vessels, Type I and Type II are probably the easiest to produce; however, as they are mainly made of metal alloy, they are strongly affected by the HE [40,41] generated by diffusion mechanisms of hydrogen into the material, as discussed in Section 3.

In this field, several studies have been carried out in the last few years with the aim of investigating the effect of hydrogen on different types of metal alloys, typically for making type I and II vessels. For example, Siddiqui and Abdullah [42] showed that in 0.31% carbon, if the hydrogenation time is increased, there will be a reduction in the ductility behavior of the material. Capelle et al. [43] carried out a burst test on notched X52 pipes after hydrogen exposure inside and outside the vessel. They showed the existence of a critical hydrogen concentration that results in a significant loss of local fracture resistance. Amaro et al. [44] formulated fatigue crack growth in X100 steel material, and Nanninga et al. [45] compared the embrittlement behavior of X52, X65, and X100 steels in a high-pressure hydrogen gas environment. They concluded that HE increased with the increase in hydrogen pressure and the alloy strength. The latter, in fact, plays an important role since lower yield strength decreases the stress concentration in the notch or crack roots due to plastic deformation. Consequently, higher stresses will be required for the crack to propagate.

Even type III vessels are affected by the discussed phenomenon due to the presence of the metallic liner.

For this reason, since the last decade, Type IV types have been largely used, especially in the automotive sector, where the weight and the tolerated pressure represent a crucial aspect.

5. Hydrogen Delivery via Pressure Pipelines

Many challenges related to the distribution and transportation of hydrogen through pipelines still need to be overcome for the widespread diffusion of hydrogen [46]. Among these, the research for the most suitable material to make pipes is certainly one of the most stimulating. Several materials can be considered; the choice depends on the type of gas pipeline (i.e., gathering, transmission, distribution, on-shore or off-shore subsea) as well as safety, durability, reliability, cost, and environmental impact [47].

The gathering and distribution pipes are generally characterized by small diameter and low pressure, and they can be made of steel, cast iron, fibrous cement, or polyethylene. The transmission tubes, on the other hand, are usually of larger diameters and pressures and are mainly made of steel.

On-shore pipes are typically made of carbon or stainless steel, whereas the off-shore ones are made of carbon or high-yield alloy steel. These pipes, however, are corrosion-susceptible as a consequence of the working environment; therefore, they must be protected from corrosion in terms of electrical insulation by external coatings in combination with cathodic protection, sacrificial anodes, or currents impressed, while the ground pipes are protected with suitable coatings, usually paint [48].

Steel pipelines have a proven experience in safety and reliability. They have been and are still used today for the distribution of natural gas and oil. The possibility of using the extensive network of steel pipelines, built over time, for the transport of blended or pure hydrogen, has been intensely explored [49]. However, the delivery of hydrogen through steel pipelines involves some problems [50]. As already observed in the previous paragraph, in fact, the presence of hydrogen in steel gives rise to the phenomenon of HE [51], which causes an increase in the probability of breakage of the material. Pipeline materials must

have particular physical properties such as strength, toughness, ductility, and weldability, as well as be economical. High-strength, low-alloy steels meet these requirements [48,52]. The life of steel pipes can be increased by protective layers such as internal and external coatings. In recent years, a number of (internal) coating techniques have been developed to prevent HE on steel [48,52,53]. Furthermore, internal hydrogen barriers using polymeric materials [53] and polymeric materials reinforced with nanomaterials [54] have also been investigated. The transmission pipes, despite being made of high-quality steel, suffer from progressive galvanic corrosion when exposed to harsh environmental conditions. Polymeric and fiber-reinforced polymer (FRP) pipelines have also been proposed as an alternative to metallic pipelines. Pipes in composite materials include a thermoplastic liner wrapped in high-strength fibers and an external protective layer.

Compared to non-reinforced polymeric pipelines, this kind of pipeline has improved burst and collapse pressure ratings, increased compression strength, tensile strength, and load-carrying capacity. The ability of FRP tubing to withstand great stresses allows for it to be coiled so that long lengths can be coiled onto a spool in an open-hole configuration. It is worth noting that the use of non-metallic pipelines for hydrogen transportation is still a relatively new technology, and further research and development are needed to fully assess the safety, reliability, and performance of these materials for hydrogen transportation. Therefore, the choice of the material should be made based on a comprehensive risk assessment and evaluation of the available options.

6. Polymers for the Hydrogen Storage and Supply

As one can observe by reading the last two sections, a big boost in the introduction of new types of vessels for storage and pipelines for the supply of hydrogen was achieved by the use of polymeric materials, which gained great attention in the development of hydrogen infrastructure due to the following versatile and extraordinary properties:

- Corrosion resistance: unlike many metals, polymers are resistant to hydrogen-induced corrosion, making them suitable for storing and transporting hydrogen safely;
- Lightweight: polymers are generally lightweight compared to metals, which can be advantageous in mobility applications, helping reduce overall vehicle weight and improve fuel efficiency;
- Design flexibility: polymers can be molded into various shapes, allowing for flexibility in design and the creation of complex sealing systems and pipes;
- No HE: research carried out by the Sandia National Laboratory in the USA [55] showed that polymers are not susceptible to HE as metals;
- Reduced permeability to hydrogen.

Thanks to these properties, polymers can offer many advantages over conventional materials in hydrogen applications, such as pipeline networks, storage areas, aerospace, fuel-cell vehicles, and hydrogen refueling stations where a number of devices, such as accumulators, valves, nozzle compressors, filters, and pre-coolers, to regulate the distribution of high-pressure hydrogen, as well as seals to reduce the risk of leaks, are involved.

Among the different types of polymeric materials, thermoplastics and elastomers are the best candidates to be used in hydrogen infrastructures [55]. Rubber/elastomeric materials, in particular, are often used as sealing devices. The reason can be attributed to their simple structure, ease of assembly and disassembly, and two-way sealing with no periodic adjustment.

Some examples of polymers that are used or being developed for hydrogen infrastructure are reported in Table 1.

Table 1. Polymers used in hydrogen infrastructure.

Abbreviation	Chemical Name
Thermoplastic	
PE	Polyethylene
HDPE	High-density polyethylene
PA PA6/PA11/12	Polyamide (nylon) Polyamide 6/Polyamide 11/Polyamide 12
PCTFE	Polychlorotrifluoroethylene
PEEK	Polyetheretherketone
PP	Polypropylene
PTFE	Polytetrafluoroethylene
Elastomers	
BR	Polybutadiene
CR	Polychloroprene
EPDM	Ethylene–Propylene Diene Monomer
EPM	Ethylene–Propylene rubber
FKM	Fluoroelastomers
HNBR	Hydrogenated Nitrile Butadiene Rubber,
IIR	Butyl rubber
MQ, VMQ, PVMQ, FMQ, FVMQ	Silicone rubbers
NBR	Nitrile rubber

Among them, PE and HDPE are widely used to line hydrogen tanks as they are lightweight, economical, and offer good chemical resistance. PA and, in particular, PA12, are of great interest as they have reduced permeability to hydrogen and thermo-mechanical properties, which allow for the pipes to withstand an operating pressure of 2 MPa. PEEK is a high-performance polymer with excellent mechanical and thermal resistance; therefore, it is used in high-quality components for the hydrogen industry. PTFE polymers are known for their high chemical and corrosion resistance, and they are used for gaskets and coatings.

NBR is resistant to hydrogen and is often used for gaskets, O-rings, and seals. It is compatible with fuels and oils but may not be suitable for extreme temperatures. FKM materials are known for their excellent chemical and thermal resistance, and they are used in gaskets, valves, and sealing components. Silicone materials are flexible and resistant to hydrogen, and they are used in low-temperature applications and as seals. In particular, VMQ has a wide temperature range and better compressive strength than MQ, which makes it suitable for some gasket applications. PVMQ has an operating temperature of approximately 100 °C lower than the MQ, with a working temperature of −100 °C that makes it suitable for low-temperature applications such as hydrogen infrastructures. FVMQ has superior chemical resistance to aggressive environments compared to other silicones, but its resistance to high temperatures is lower.

However, polymers also have some limitations and challenges, such as mechanical integrity, due to the exposition to high-pressure hydrogen, aging phenomena, rapid decompression, material selection, design optimization, and recycling.

All of these criticisms are mainly linked to the gas permeability mechanisms that are particularly enhanced in elastomeric materials as a consequence of their amorphous microstructures. In fact, as hydrogen is a small molecule in nature, it is quite easy for it to permeate within the polymeric chains, and this, if not controlled/predicted, can lead to catastrophic failure. In the next section, the phenomenology of gas permeability will be discussed, also considering the main effects that can affect it.

7. Gas Permeation in polymers

It is well known that polymers are permeable to gases [56]. As hydrogen molecules are very small, they can easily dissolve in the material and diffuse through it. If one wants to understand the physics that involves the permeation behavior through polymers, a solution diffusion mechanism can be used. Basically, the permeation of hydrogen in a polymer involves two mechanisms: (i) hydrogen dissolution at the free surface of the material; and (ii) diffusion inside the material [57]. Flaconneche et al. [58] described the transport process by considering three main consecutive stages, as reported below:

1. Absorption of the gas on the high-pressure side due to the chemical affinity;
2. Diffusion of the gas inside the polymer;
3. Desorption of the gas on the low-pressure side;

This process is schematically described in Figure 4. Within this Figure, the black solid curve represents the gas concentration gradient, and C_H and C_L represent the gas concentration on the high-pressure and low-pressure sides, respectively.
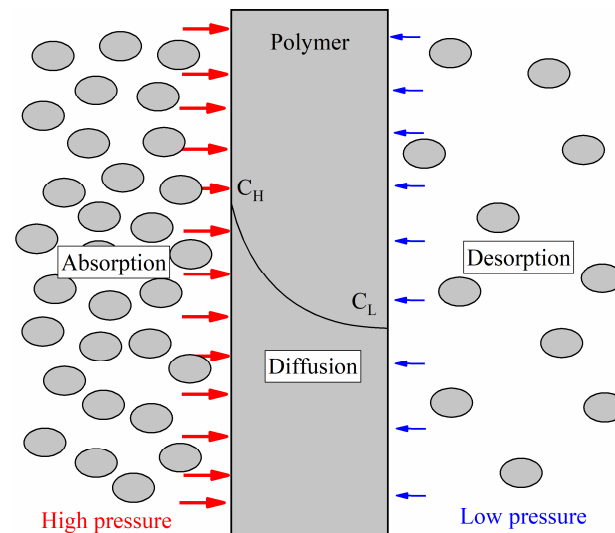
Figure 4. Schematic illustration of gas transport through polymers.

The gas permeation process can be characterized by three main physical properties: solubility (S, mol/m^{3}Pa); diffusivity (D, m^2/s); and permeability (P, molm/m^{2}sPa). Solubility represents the gas quantity that the material can absorb. Diffusivity is a kinetic property that describes the velocity by which the gas moves between a point with high pressure and a point characterized by lower pressure. Finally, the permeability represents the capability of the gas to move within the polymeric material. Actually, there is a relationship that correlates all of these coefficients, and it can be expressed as Equation (1):

$$P = S \times D \tag{1}$$

The dominant parameter of permeation is gas diffusion, which is very slow [56]. It was observed that diffusion existed only in the amorphous regions of a polymer and it was very limited in the crystalline ones [59]. Gas molecules can diffuse through the polymer by taking advantage of the free volume created by the chain segment motion in the polymer [60].

In order to estimate the hydrogen permeability, diffusivity, and solubility coefficients on a material, a proper experiment, according to Standard ISO 11114-5 [61] and named high-pressure hydrogen gas permeation test (HPHP), can be carried out. The experimental setup, as reported in Figure 5, is made of high-pressure and low-pressure sealing cavities, sealing rings, a wire mesh, and a sintered metal plate. The sample is clamped between the two sealed chambers, and the sintered metal plates are applied to support the sample in order to prevent possible deformation during the experiment. The wire mesh is used to avoid direct contact between the sintered metal and the sample surface and to ensure an even distribution of the hydrogen on the sample during the test.
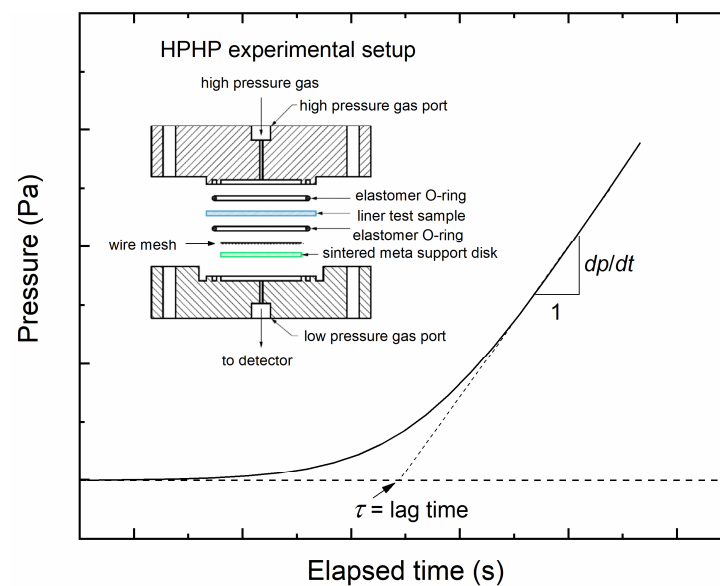
Figure 5. Schematic representation of the permeability test.

The HPHP allows us to estimate the permeability coefficient of the material by measuring the quantity of gas/hydrogen that permeates the low-pressure chamber.

In particular, hydrogen is injected into the upper chamber under vacuum. The pressure in the upper chamber increases, and then, hydrogen gas starts to permeate through the specimen. Diffusion mechanisms within the material start, and at a certain time, some hydrogen molecules go inside the lower-pressure chamber. At this stage, the pressure in the lower chamber increases because the higher quantity of hydrogen gas diffused within the polymer comes inside the lower-pressure chamber. After some time, hydrogen gas permeating through the sample is constantly released, and the pressure increases linearly with the elapsed time. A typical curve, in terms of pressure measured at the low-pressure chamber as a function of the elapsed time, is reported in Figure 5.

As one can observe, at the beginning of the experiment, the pressure is null, as no molecules exist in the lower-pressure chamber. Then, as soon as gas molecules diffuse and go inside the lower-pressure chamber, pressure increases until the process saturates, and the slope of the pressure becomes constant. The latter can be fitted with a straight line, and the time lag τ, representing the point where the fitted line intersects the initial pressure, can be obtained.

At this stage, the diffusivity (D) can be calculated as follows:

$$D = \frac{l^2}{6\tau} \tag{2}$$

where l is the sample thickness (m), and τ is the lag time (s). The permeability coefficient (P) can be obtained as follows:

$$P = \frac{V_C}{RTp_hA} \cdot \frac{dp}{dt} \tag{3}$$

where T and R are the temperature and gas constants, respectively; A is the area of the specimen; V_C is the volume of the low-pressure chamber; p_h is the pressure of hydrogen in the high-pressure chamber, and dp/dt is the slope of the curve, as reported in Figure 5. Once the diffusivity (D) and permeability (P) are measured, the solubility coefficient (S) can be calculated according to Equation (1).

It is important to underline that permeability is strongly temperature- and pressure-dependent; therefore, it is of great interest to know how it changes, especially if one considers that polymers operating in a hydrogen environment must work in different thermo-mechanical conditions. More details are reported in the next two sections.

8. Effect of Temperature on Hydrogen Permeability in Polymers

According to ISO 19881 standards [62], the maximum temperature that hydrogen should reach in the storage system cannot be higher than 85 °C [63]. For this reason, in some applications, it is typically pre-cooled at a temperature of −40 °C. In this way, overheating phenomena can be avoided [64].

Such temperature variations, from −40 °C to 85 °C, can be critical for a hydrogen storage cylinder; therefore, it is extremely important to understand how it can influence the hydrogen transport properties of the polymer.

In early theoretical studies [58], it was shown that permeability *P*, diffusion *D*, and solubility *S* of polymers followed the Arrhenius' law, as described by the following equations:

$$S(t) = S_0 \cdot \exp\left(-\frac{\Delta H_S}{RT}\right) \tag{4}$$

$$D(t) = D_0 \cdot \exp\left(-\frac{E_D}{RT}\right) \tag{5}$$

$$P(t) = P_0 \cdot \exp\left(-\frac{E_P}{RT}\right) \tag{6}$$

where S_0, D_0, and P_0 are the limit values of the corresponding coefficient when the temperature, theoretically, approaches infinity.

ΔH_S is the apparent activation energy of the heat of dissolution; E_D is the apparent activation energy of the heat of diffusion, and E_P is the permeation that the gas needs to dissolve within the polymer. According to Equation (1), it is possible to write that $E_P = \Delta H_S \cdot E_D$; therefore, one can state that for hydrogen, both ΔH_S and E_D are positive [65]. This means that for a specific pressure value, the hydrogen permeation increases according to the temperature.

In the field of polymeric materials, a very interesting study aimed at analyzing the temperature dependence of hydrogen permeability on polymers was conducted by Barth et al. [55]. In particular, they studied this phenomenon on both thermoplastic and elastomeric materials, such as HDPE, PA, PVC, butyl rubber, etc. What they observed is shown in Figure 6.
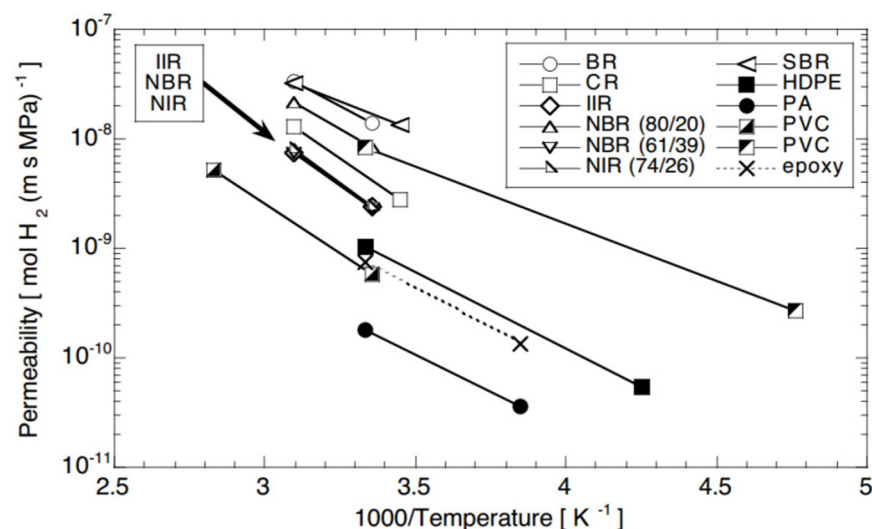

Figure 6. Temperature dependence of hydrogen permeability of several polymer materials. Data are collected from the following references: BR, IIR, NBR, NIR [66]; CR, SBR [67]; HDPE, PA, epoxy, PVC (low temp. range) [68]; PVC (high temp. range) [69].

The graph reports the permeability coefficient in the logarithm scale as a function of the reciprocal of temperature for different investigated materials. The linear trend

demonstrates that the hydrogen permeability follows Arrhenius' law with the temperature. Please consider that, for schematic purposes, within this Figure, only two labels per line are reported, but, actually, each line is the fitting of multiple points (see refs. [55]). Results also revealed that there is an order of magnitude difference between 85 °C and the room temperature and that at a temperature lower than room temperature, the permeation reduction is relatively smaller, in the order of 2%.

Additional studies aimed at investigating the effect of temperature on the permeability of polymers were carried out by Yu Sun [65]. In this study, the authors carried out experiments on PA6 and LIC/PA6 materials at different temperatures (-10 °C, 25 °C, 85 °C) and pressures (25–50 MPa).

Figure 7, like the previous one, reports the permeability coefficient in the logarithm scale as a function of the reciprocal of temperature for the two materials. The obtained results show the same trend reported by Barth et al. [55].
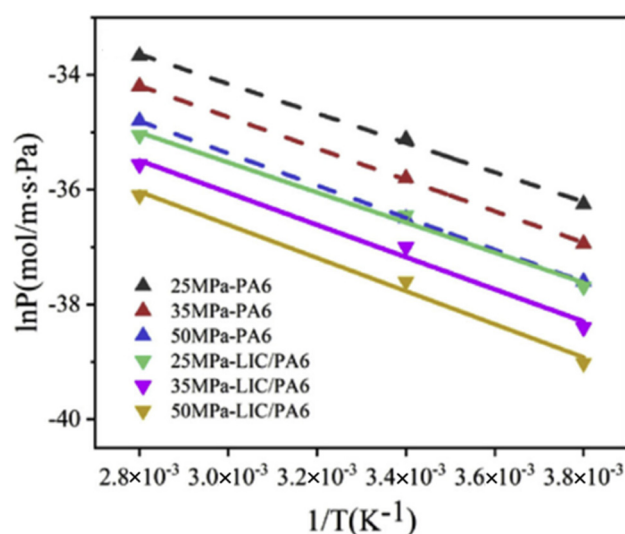
Figure 7. The relationship between hydrogen permeability coefficient and temperature of PA6 and LIC/PA6 [65].

Finally, a similar investigation was conducted by Rogers [70] on HDPE. The same conclusions, reported in previous studies, were obtained.

From a physical/chemical point of view, the permeability of polymers increases with increasing temperature for several reasons. First, the solubility coefficient increases with the temperature because the polymer chains expand and create more free volume for the penetrant to dissolve. The free volume is the space between the polymer chains that can accommodate the gas or liquid molecules. The free volume increases with the temperature due to the thermal expansion and the increased chain mobility of the polymer [71].

Second, the diffusion coefficient increases with the temperature because the polymer chains become more flexible and allow for the penetrant to diffuse faster. The diffusion of the penetrant in the polymer is governed by Fick's law, which states that the flux of the penetrant is proportional to the concentration gradient and the diffusion coefficient. The diffusion coefficient depends on the molecular size and shape of the penetrant, the molecular weight and structure of the polymer, and the temperature of the system. The diffusion coefficient increases with the temperature due to the Arrhenius equation, which states that the diffusion coefficient is proportional to the exponential ratio of the activation energy and the temperature. The activation energy is the energy barrier that the penetrant has to overcome to move from one position to another in the polymer matrix. The activation energy decreases with the temperature due to the increased chain mobility and free volume of the polymer [71].

Third, the permeability of polymers increases with the temperature because the material tends to approach the glass transition temperature (T_g). The T_g is the temperature at

which the polymer changes from a rigid and glassy state to a flexible and rubbery state. Above T_g, the polymer chains have more mobility and free volume, which facilitate the solubility and diffusion of the penetrant in the polymer. Below T_g, the polymer chains are more constrained and have less free volume, which hinders the solubility and diffusion of the penetrant in the polymer. Therefore, the permeability of polymers increases when $T \to T_g$ for $T < T_g$ [71].

9. Effect of Pressure on Hydrogen Permeability in Polymers

Gas pressure is an additional parameter that has a strong influence on the transport properties of polymeric material.

In order to study how the polymer hydrogen permeability of HDPE can be modified when high pressure is applied, Fujiwara et al. [72] used the HPHP method. The analysis was carried out considering pressure values in the range of 10–90 MPa. In their conclusion, the authors observed that all the hydrogen transport coefficients decreased with the increasing of the applied pressure, even though among them, the decreasing rate of the diffusion was higher than the solubility, indicating that after a specific temperature value, hydrogen permeation was mainly affected by diffusion rather than solubility.

The effect of pressure on hydrogen permeability was also investigated by Yu Sun [65] on PA6 and LIC/PA6 materials. Three different pressure values were analyzed, i.e., 25–35–50 MPa. Figure 8 reports the logarithm of the hydrogen permeability as a function of the applied pressure for the two materials, showing a linear decrease in this scale with the increase in the pressure. However, it is important to underline that these measurements were carried out after decompression, and this can be strongly linked to internal damages induced by mechanical stress. More details about the decompression process will be discussed in the following sections.
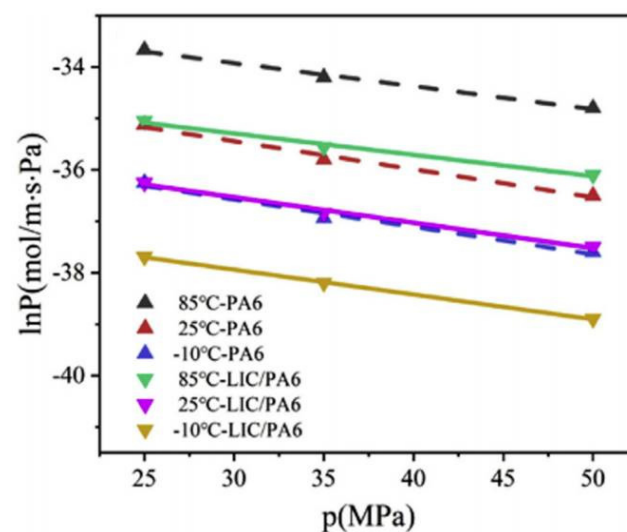
Figure 8. The relationship between hydrogen permeability coefficient and pressure of PA6 and LIC/PA6 [65].

The observation reported in the literature can be explained as a consequence of the following events: (i) higher pressures induce the polymer to obtain a most compact configuration; (ii) high compactness means an increase in the density; (iii) high density means reduction in the free volume; (iv) less free volume means lower diffusion [73,74]. Even in the case of thermoplastic polymers, as reported by Fumitoshi et al. [75], in polyethylene material, a high-pressure hydrogen environment induces the crystallinity to increase with a consequent reduction in hydrogen diffusion. However, it is important to point out that this change in crystallinity is reversible. In fact, when the high applied pressure is removed, the polymer's crystallinity returns to its original value.

Now, the question is, how can the pressure and permeability variation influence the mechanical performances of polymeric materials? In this case, it is important to distinguish between thermoplastics and elastomers. In fact, as a consequence of their microstructure, hydrogen has a different impact.

As previously discussed, the free volume within the polymer and the segmental mobility of the polymer chains influence the transport properties of hydrogen and gas, in general.

Elastomers, in fact, are characterized by a bigger free volume, allowing for easy diffusion through the polymer chains compared to glassy polymers characterized by a semi-crystalline microstructure. The high degree of crystallinity in thermoplastics can result in lower permeability of hydrogen compared to elastomers. As previously discussed, even T_g can affect transport properties; in fact, higher T_g materials can be less affected by gas permeation.

Studying the effect of both hydrogen environments combined with the high pressure is not an easy task; in fact, special facilities with special security systems are required. Actually, there are some French [76] and Italian research groups [77] that developed a setup able to execute mechanical tests in hydrogen environments under pressure. However, in the first case, only low pressure can be investigated, whereas in the latter case, the high-pressure opportunity exists, but only preliminary tests on metals have been performed up to now.

In the published literature, there are relatively little data characterizing the mechanical properties of polymers/materials in the presence of both hydrogen and high pressure (up to 70–100 MPa).

Instead, there are several studies where the only effect of the high hydrostatic pressure on the mechanical behavior of polymers is investigated. Reported experiments consist of stress–strain measurements on thermoplastic materials under tension, compression, or torsion within an enclosed pressure chamber. Results obtained by scholars reveal that the hydrostatic pressure increases the elastic modulus, the strength, and the final elongation, and it also has beneficial effects on crack propagation.

To our knowledge, one of the first works where the effect of pressurized hydrogen on the mechanics of thermoplastic polymers was investigated was made by Castagnet et al. [76].

In their first study, the influence of coupling between gas diffusion and tensile properties was investigated in PE- and PA11-based materials. Samples were tested in atmospheric air as well as in hydrogen, with a test pressure of 3 MPa. From their experiments, they concluded that tensile properties were not affected by H_2 diffusion. In a further study, Castagnet et al. [78] also investigated the effect of long-term aging on PE- and PA11-based material. After 13 months in hydrogen at different pressures, 2 and 5 MPa, and temperatures below and above the glass transition, no deleterious effect was observed on the mechanical properties of PE and PA11.

In addition, a hydraulic testing machine was fitted within the pressure hydrogen chamber to investigate not only the monotonic properties and long-term creep but also ductile fracture in PE and PA11 [79]. They concluded that tensile, static properties, such as the elastic modulus and the yield stress, viscous creep deformation, and ductile fracture, were not highly modified by hydrogen permeation.

In 2014, Alvine et al. [80] conducted the in situ tensile test of polymer materials under a hydrogen pressure greater than 10 MPa. They find that high-pressure (35 MPa) hydrogen significantly reduces the tensile strength of HDPE (about 10%).

Research studies focused on the effects of high-pressure hydrogen on sealing materials are relatively new.

In this context, Yamabe et al. [81,82] produced NBR and EPDM made by different carbon black and silica percentages with the aim of analyzing how the high-pressure hydrogen modified the penetration properties and hydrogen content of the materials. However, it is important to underline that experiments were performed ex situ; i.e., the materials were

preliminarily exposed to high-pressure hydrogen (100 MPa) at room temperature and then tested in a laboratory environment. It is shown that as the volume increases, the elastic modulus and tensile strength of the samples decrease, which is significantly attributed to the decrease in the cross-link density and elongation of NBR rubber.

Menon et al. [83] exposed a select group of two elastomers (NBR and Viton A®) and two thermoplastics (HDPE, PTFE) to hydrogen in static conditions at a pressure of 100 MPa at ambient temperature for a week in order to estimate the influence of hydrogen exposure on properties such as the modulus, T_g, compression set properties, density, outgassing characteristics, and the tensile strength. They observed that thermoplastics did not experience any significant change in major physical properties, whereas the elastomers showed very significant variations.

Most recently, Theiler et al. [84] investigated the influence of a high-pressure hydrogen environment on the physical and mechanical properties of two types of cross-linked hydrogenated acrylonitrile butadiene rubbers. In particular, they exposed the materials to hydrogen up to 100 MPa at 120 °C for 7 and 21 days and observed a decrease in density and mechanical properties immediately after exposure, even though the materials recovered their original values after 48 h.

10. Ways to Manage Permeability in Polymers

Gas permeability is a crucial material property to take into account when dealing with the use of polymers in hydrogen infrastructures. Designers would like to keep this parameter as low as possible, meaning that neither diffusivity D or solubility S exhibit low values in the operating conditions. For that reason, semicrystalline polymers, as a consequence of their morphology, are the most appropriate. In fact, the hydrogen permeability of polymers decreases with increasing polymeric crystallinity, as the crystalline regions of the polymer have lower free volume and higher density than the amorphous regions, which hinder the diffusion and solubility of hydrogen in the polymer. Michaels and Parker [85] and Michaels and Bixler [59,86] demonstrated that for isotropic HDPE, the sorption and the diffusion took place only in the amorphous regions of the material. The crystalline zones, in fact, can be considered as an inaccessible volume for the sorption process, and it drastically reduces the diffusion phenomenon. Therefore, it is quite clear that the first parameter to consider to control the barrier properties of polymeric materials is their chemical structure.

The T_g of the polymer is another important factor that affects the hydrogen permeability of the polymer. In fact, at a certain operating temperature, being far below T_g will guarantee lower permeability of the material. Therefore, it is always convenient to use materials with high T_g.

An additional way to control/improve the hydrogen barrier properties of the polymer is to add fillers within the material. By making a physical barrier in the polymer, fillers create a tortuous path for the hydrogen molecules to penetrate the polymer matrix, as Figure 9 illustrates. Such a phenomenon was physically observed by Yu Sun [65] by adding fillers within PA6. In addition, he showed that the introduction of filler also increased the stiffness of the material, and the flexibility of the polymer chain decreased, making it more difficult for hydrogen molecules to penetrate the polymer.

The effect of filler on the hydrogen permeability of EPDM composite polymers was also investigated by Yamabe et al. [81,82] and Nishimura [87]. They observed that silica-filled EPDM composites exhibited a much lower amount of absorbed hydrogen content, demonstrating that the addition of silica is an effective way to enhance the resistance to high-pressure hydrogen gas of rubber composites.

Sun et al. [65] added lamellar silicate nanofiller (LIC) to a PA6 grade material and investigated the hydrogen permeability in different operating pressure levels (25 MPa, 35 MPa, 50 MPa) and temperature conditions (−10 °C, 25 °C, 85 °C). They observed that compared with the base material, i.e., the non-filled one, the hydrogen barrier properties in

filled grades were 3–5 times higher. In addition, a bigger improvement in the lower range of temperatures was observed as a consequence of the lower mobility of polymeric chains.
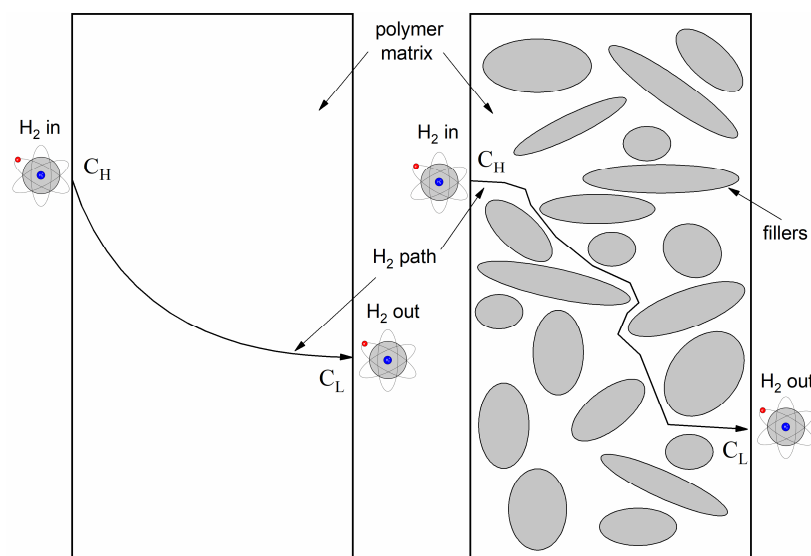
Figure 9. Schematic representation of H$_2$ path during the diffusion process within a polymeric matrix with no fillers (**left**) and with fillers inside (**right**).

Graphene nanosheets are also a type of fillers that can enhance the mechanical properties of polymers, but they are prone to agglomeration, so they need surface functionalization to improve the separation of the sheets and the insertion of polymer chains [88–90]. A better filler distribution can reduce the filler agglomerations and lead to better mechanical properties.

Recently, even carbon nanotubes (CNT) were investigated by Takeyama et al. [91] as possible fillers to improve the performances of elastomers used in high-pressure hydrogen environments. In particular, they exposed an NBR material filled with CNT to high-pressure hydrogen (30 to 90 MPa) with the aim of investigating the relationship between the amount of hydrogen intrusion and the volume variation. It was found that the balance between the amount of hydrogen intrusion and the volume change due to exposure to high-pressure hydrogen can be improved by using CNTs.

In the next sections, the damage mechanisms of polymers, mainly related to the material permeability operating in a hydrogen environment, are reported and described.

11. Rapid Gas Decompression in Polymers: The Phenomenology

Rapid gas decompression (RGD) is a phenomenon that occurs when a high-pressure gas, such as hydrogen, is suddenly released from a confined space, such as a vessel or a pipe. RGD can cause severe damage to the materials that are in contact with the gas, especially polymers and composites, which are widely used for hydrogen storage and transport applications. RGD can induce different types of damage mechanisms, such as cavitation, blistering, cracking, delamination, and rupture, depending on the gas pressure, temperature, decompression rate, and material properties [92].

The main cause of RGD damage is the gas diffusion and desorption process in the polymer matrix. Under high pressure, gas molecules can penetrate into the polymer and occupy the free volume between the polymer chains. When the gas pressure is rapidly reduced, the gas molecules inside the polymer tend to escape and reach a new equilibrium with the external pressure. However, the gas diffusion and desorption rates are limited by the polymer viscosity and permeability, which depend on the polymer T_g, crystallinity, cross-linking, and plasticization. Therefore, the gas pressure inside the polymer can be higher than the external pressure for a certain time, creating a pressure gradient that can exceed the material strength and cause damage [92].

The extent and severity of RGD damage depend on several factors, such as the gas type, the gas solubility, diffusion coefficients in the polymer, the initial gas pressure and temperature, the decompression rate and profile, the polymer type and grade, the polymer thickness and geometry, and the polymer mechanical properties.

RGD damage can compromise the performance and safety of hydrogen vessels and pipes, and, thus, it should be prevented or minimized by proper design and material selection.

The possible strategies to reduce RGD damage are directly linked to the following permeability properties of the polymers: choosing polymers with high T_g, high crystallinity, high cross-linking, and low gas solubility and diffusion coefficients; using multilayer or composite structures with gas barrier layers or coatings; controlling the gas pressure, temperature, and decompression rate and profile; and adding additives or modifiers to the polymer to improve its gas resistance and compatibility.

12. Damages Induced by RGD

The literature on rapid hydrogen decompression is not extensive. The damage mechanisms induced by RGD of hydrogen were properly described and modeled in [82] under a single exposure to high-pressure hydrogen.

When a rubber is exposed to hydrogen gas, supersaturated hydrogen molecules cluster in micrometer-sized bubbles (Figure 10) [82]. The latter represent stress concentration sites for the material that, after several filling and emptying cycles, will generate blisters (cracks) (see Figure 10). Internal damage may increase the gas permeation, as the inner local defects can represent preferential diffusion paths that promote gas transport [93].
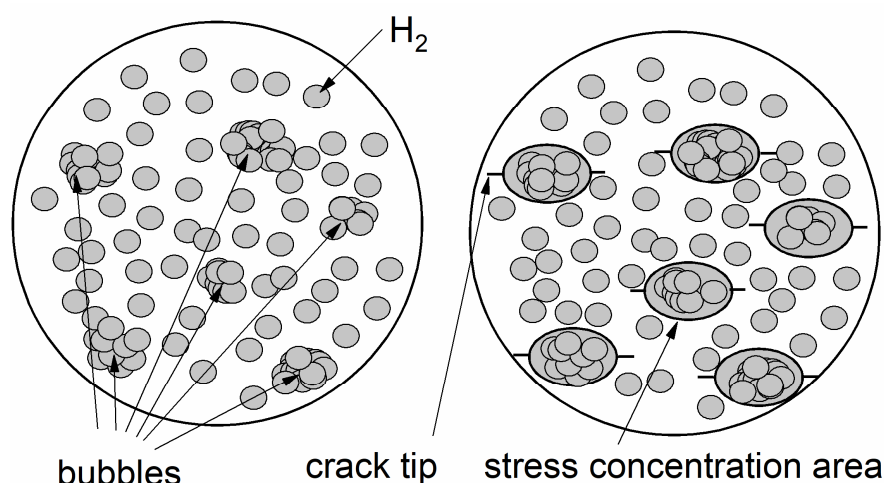
Figure 10. Schematic representation of fillers within polymeric chains.

The first works where the effect of RGD on elastomers was extensively investigated were proposed by Yamabe et al. [82,94,95], where EPDM, VMQ, and HNBR were decompressed from 10 MPa of hydrogen pressure. The aim was to investigate the effect of different fillers on the blistering mechanisms. What the authors observed was that induced damages were less critical in silica-filled composites than in elastomers without fillers. In addition, they also observed that in EPDM material, cracks were generated when decompression was carried out at a pressure higher than 2 MPa.

Jaravel et al. [96,97] characterized a modified silicon elastomer decompressed from hydrogen pressures up to 27 MPa. Transparent specimens were used to visually track damages during the experiment. They found that higher saturation pressures and faster decompression rates facilitate blistering; the presence of tensile stresses within the sample accelerates the damage process; the elastomer does not exhibit damage phenomena at decompression rates below 0.2 MPa/min for low saturation pressure, and the decompression rate can be increased by decreasing the saturation pressure [97].

Kane-Diallo et al. [98] carried out tests to identify how the applied pressure (7–15 MPa) and the decompression rate (0.75–30 MPa/min) influenced damage generation. By using transparent EPDM (unfilled) samples, they also visually tracked damages during the experiment and used this information to model and predict damage phenomena. Based on in situ captured images, it appears that cavity size increases with rising saturation pressure and decompression rate.

Notably, thermoplastic polymers are also susceptible to the RGD process. Existing research predominantly focuses on HDPE and PA materials commonly used for lining applications. Yersak et al. [99] and Baldwin [100] exposed specimens of HDPE and PA grades to 87.5 MPa and 65 MPa of high-pressure hydrogen, respectively, and upon the RGD, they observed cavitation damage.

Similarly, in semi-crystalline materials, RGD is a diffusion-controlled phenomenon, implying that cavitation may persist even after decompression [101]. Ono et al. [102] conducted experiments on an HDPE grade exposed to 90 MPa of high-pressure hydrogen, identifying internal damage initiation caused by RGD. Their findings quantitatively reveal the evolution of internal damage due to cyclic high-pressure exposure. In addition, thanks to optical investigation of the cross-section, they observed that damages induced by RGD were mainly concentrated in the middle of the specimen [102].

An additional damage mechanism that may occur in thermoplastic material is represented by the liner collapse with a permanent deformation (see Figure 11). Research shows that the ratio of material yield stress to Young's modulus ratio determines the critical pressure for liner collapse [103].
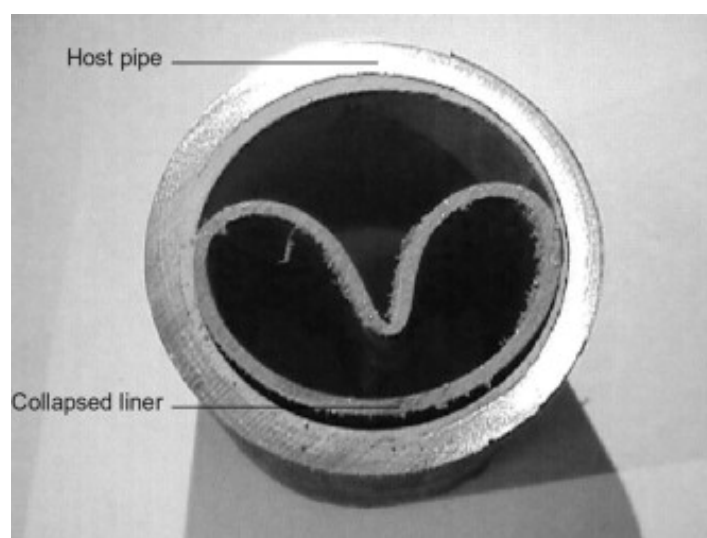
Figure 11. Example of liner collapse in a pressure vessel [104].

The liner collapse behavior, which may occur during the compression and decompression stages, was tested on a laboratory scale by Pepin et al. [105,106]. Considering that a full-scale experiment such as this one was quite complex and expensive, they developed a laboratory-scale liner collapse test method. A thermoplastic polymer (PA 6, Tg42C) plate was used as the liner material, and tests were carried out at a maximum hydrogen pressure of 30 MPa at 50 °C in an autoclave. They identified key parameters to develop models to predict such a catastrophic damage mechanism [105].

13. Aging in Polymers: The Phenomenology

The hydrogen aging phenomenon is the degradation of the mechanical properties of polymers due to exposure to hydrogen gas at high pressure and temperature. Hydrogen aging can affect different characteristics of the material, such as strength, stiffness, toughness, ductility, and fatigue resistance, depending on the polymer type, structure, and

morphology. Hydrogen aging can also induce damage such as cracking, blistering, HE, and swelling, depending on the hydrogen solubility, diffusion, and desorption in the polymer matrix [107–109].

The main cause of this phenomenon is the interaction of hydrogen molecules with the polymer chains. Hydrogen molecules, in fact, can penetrate the polymer and occupy the free volume between the polymer chains, whose size depends on the T_g, crystallinity, cross-linking, and plasticization of the material. The free volume decreases with the increase in these factors, which results in lower hydrogen solubility and diffusion in the polymer [108,109].

The hydrogen molecules inside the polymer can cause two types of effects: physical; and chemical. The physical effect is the creation of a pressure gradient between the polymer and the external environment, which can cause the polymer to expand or contract. The expansion or contraction of the polymer can result in mechanical stresses and strains, which can affect the mechanical properties and induce damage to the polymer. The chemical effect is the formation of chemical bonds between the hydrogen molecules and the polymer chains, which can alter the molecular structure and morphology of the polymer. The chemical bonds can be either reversible or irreversible, depending on the type and strength of the bonds. The reversible bonds can be broken by increasing the temperature or decreasing the pressure, while the irreversible bonds can only be broken by chemical reactions. The chemical bonds can affect the mechanical properties and induce damage to the polymer by changing the chain mobility, cross-linking, and crystallinity [107–109].

14. Damages Induces by Aging

In recent years, some attempts to investigate the effect of hydrogen aging on polymers have been made. In particular, concerning the elastomeric materials, Yamabe et al. [110] exposed NBR material grade to 100 MPa-pressure hydrogen and did not observe any particular changes in the T_g of the material. The same result was obtained by Menon et al. [83] on the NBR grade, whereas a reduction in the T_g of the FKM grade was measured after high-pressure hydrogen exposure due to the reduced crystallinity. Fujiwara et al. [111] carried out cyclic high-pressure (90 MPa) hydrogen exposure at 30 °C on CB-filled and NBR-grade-filled, and also, in this case, no structural changes were observed after the treatment.

Concerning thermoplastic materials, the trend is a bit different. In fact, Menon et al. [83] investigated the aging phenomenon of PTFE at 100 MPa and room temperature. After one week of hydrogen exposure, the material, compared with the non-exposed one, showed an increase in the elastic modulus, the yield stress, and the strength. Instead, Castagnet et al. [76,78,79] investigated PA grade and PA11 grade by exposing them to hydrogen at different pressures (0.5–3 MPa) and different temperatures (20–80 °C) for 13 months. No modifications in the mechanical properties were observed. Finally, Alvine et al. [80] carried out an aging test on HDPE by exposing it to hydrogen at different pressures (28, 31, and 35 MPa), and they obtained a reduction in the tensile strength.

Based on these observations, we can state that the hydrogen aging phenomenon can compromise the performance and durability of polymers used for hydrogen storage and transport applications, and, thus, it should be prevented or minimized by proper design and material selection. However, a mismatch among the obtained data still exists; therefore, many efforts have to be made in order to better understand this detrimental phenomenon.

15. Summary

This article reports the results of an in-depth bibliographic investigation on the effects of hydrogen permeability of polymeric materials and polymer-based materials used for hydrogen storage and distribution infrastructures. In particular, the influence of permeability on the mechanical properties and the induced mechanisms that generate damage in the case of cyclic depressurization and aging are investigated.

The analysis highlighted that many studies have been conducted on the influence of pressure and temperature on permeability when they act separately and independently.

Both thermoplastic and elastomeric materials have been studied. It has been found, in general, that increasing pressure reduced permeability, whereas temperature induced an increase. Finally, an inverse correlation between permeability and mechanical properties as pressure varied has been experimentally demonstrated.

16. Conclusions

Based on the reported literature, one can state that more studies that correlate permeability and mechanical properties as temperature varies are needed. More thermoplastic polymers and their composites can and/or must be tested in order to broaden the range of materials that can be selected in the design phase. The same could be performed for elastomers, focusing on the possibility of developing new types of reinforced elastomers with low permeability and also using innovative forms of reinforcement, such as graphene and nanotubes.

Concerning damage caused by the rapid decompression of hydrogen, it must be noted that the literature is not very extensive on this topic, and even if the mechanisms of induced damage have already been well described and modeled, further experimental studies must be conducted to better understand the mechanisms that determine its development.

Finally, it should be highlighted that, unfortunately, studies on the behavior of the material under the simultaneous action of pressure and temperature are completely lacking in the literature. Its knowledge could be crucial to avoid catastrophic events during the filling and emptying processes of hydrogen storage and distribution systems. Currently, only a few laboratories in the world are able to perform these types of tests. Therefore, further investigation is warranted. Further efforts and huge investments are needed for the development of new experimental apparatus in order to accelerate studies on the behavior of polymers operating in the most critical environmental conditions (high pressure and temperature for a long time) in the presence of hydrogen. It can be hoped, in this way, that the results obtained will make it possible to develop design methodologies for the safe storage and transport of hydrogen.

References

1. Panos, E.; Densing, M.; Volkart, K. Access to electricity in the World Energy Council's global energy scenarios: An outlook for developing regions until 2030. *Energy Strategy Rev.* **2016**, *9*, 28–49. [CrossRef]
2. Armaroli, N.; Balzani, V. Towards an electricity-powered world. *Energy Environ. Sci.* **2011**, *4*, 3193. [CrossRef]
3. Capellán-Pérez, I.; Arto, I.; Polanco-Martínez, J.M.; González-Eguino, M.; Neumann, M.B. Likelihood of climate change pathways under uncertainty on fossil fuel resource availability. *Energy Environ. Sci.* **2016**, *9*, 2482–2496. [CrossRef]
4. Mahmud, M.A.P.; Lee, J.; Kim, G.; Lim, H.; Choi, K.-B. Improving the surface charge density of a contact-separation-based triboelectric nanogenerator by modifying the surface morphology. *Microelectron. Eng.* **2016**, *159*, 102–107. [CrossRef]
5. Turconi, R.; Boldrin, A.; Astrup, T. Life cycle assessment (LCA) of electricity generation technologies: Overview, comparability and limitations. *Renew. Sustain. Energy Rev.* **2013**, *28*, 555–565. [CrossRef]
6. Jacobson, M.Z.; Delucchi, M.A.; Bazouin, G.; Bauer, Z.A.F.; Heavey, C.C.; Fisher, E.; Yeskoo, T.W. 100% clean and renewable wind, water, and sunlight (WWS) all-sector energy roadmaps for the 50 United States. *Energy Environ. Sci.* **2015**, *8*, 2093–2117. [CrossRef]
7. Hertwich, E.G.; Gibon, T.; Bouman, E.A.; Arvesen, A.; Suh, S.; Heath, G.A.; Bergesen, J.D.; Ramirez, A.; Vega, M.I.; Shi, L. Integrated life-cycle assessment of electricity-supply scenarios confirms global environmental benefit of low-carbon technologies. *Proc. Natl. Acad. Sci. USA* **2015**, *112*, 6277–6282. [CrossRef]
8. Latunussa, C.E.L.; Ardente, F.; Blengini, G.A.; Mancini, L. Life Cycle Assessment of an innovative recycling process for crystalline silicon photovoltaic panels. *Sol. Energy Mater. Sol. Cells* **2016**, *156*, 101–111. [CrossRef]

9. Ling-Chin, J.; Heidrich, O.; Roskilly, A.P. Life cycle assessment (LCA)—From analysing methodology development to introducing an LCA framework for marine photovoltaic (PV) systems. *Renew. Sustain. Energy Rev.* **2016**, *59*, 352–378. [CrossRef]

10. Li, Z.; Du, H.; Xiao, Y.; Guo, J. Carbon footprints of two large hydro-projects in China: Life-cycle assessment according to ISO/TS 14067. *Renew. Energy* **2017**, *114*, 534–546. [CrossRef]

11. Hou, G.; Sun, H.; Jiang, Z.; Pan, Z.; Wang, Y.; Zhang, X.; Zhao, Y.; Yao, Q. Life cycle assessment of grid-connected photovoltaic power generation from crystalline silicon solar modules in China. *Appl. Energy* **2016**, *164*, 882–890. [CrossRef]

12. Luo, W.; Khoo, Y.S.; Kumar, A.; Low, J.S.C.; Li, Y.; Tan, Y.S.; Wang, Y.; Aberle, A.G.; Ramakrishna, S. A comparative life-cycle assessment of photovoltaic electricity generation in Singapore by multicrystalline silicon technologies. *Sol. Energy Mater. Sol. Cells* **2018**, *174*, 157–162. [CrossRef]

13. Asdrubali, F.; Baldinelli, G.; D'Alessandro, F.; Scrucca, F. Life cycle assessment of electricity production from renewable energies: Review and results harmonization. *Renew. Sustain. Energy Rev.* **2015**, *42*, 1113–1122. [CrossRef]

14. Fragiacomo, P.; Genovese, M. Technical-economic analysis of a hydrogen production facility for power-to-gas and hydrogen mobility under different renewable sources in Southern Italy. *Energy Convers. Manag.* **2020**, *223*, 113332. [CrossRef]

15. Fragiacomo, P.; Piraino, F. Numerical modelling of a PEFC powertrain system controlled by a hybrid strategy for rail urban transport. *J. Energy Storage* **2018**, *17*, 474–484. [CrossRef]

16. Sun, Z.; Luo, E.; Meng, Q.; Wang, X.; Ge, J.; Liu, C.; Xing, W. High-Performance Palladium-Based Catalyst Boosted by Thin-Layered Carbon Nitride for Hydrogen Generation from Formic Acid. *Acta Phys.-Chim. Sin.* **2022**, *38*, 2003035. [CrossRef]

17. Iulianelli, A.; Al-Muhtaseb, A.H.; Spazzafumo, G. Preface to the special issue dedicated to the Hydrogen Power Theoretical and Engineering Solutions International Symposium (HYPOTHESIS)—XVI Edition. *Renew. Energy* **2023**, *206*, 767–768. [CrossRef]

18. Amin, M.; Shah, H.H.; Fareed, A.G.; Khan, W.U.; Chung, E.; Zia, A.; Farooqi, Z.U.R.; Lee, C. Hydrogen production through renewable and non-renewable energy processes and their impact on climate change. *Int. J. Hydrogen Energy* **2022**, *47*, 33112–33134. [CrossRef]

19. Fragiacomo, P.; Genovese, M. Modeling and energy demand analysis of a scalable green hydrogen production system. *Int. J. Hydrogen Energy* **2019**, *44*, 30237–30255. [CrossRef]

20. Herkel, S.; Meyer, R.; Gerhardt, N. Hydrogen technologies in buildings. In *Hydrogen Technologies*; Springer International Publishing: Cham, Switzerland, 2022; pp. 151–169. [CrossRef]

21. Fragiacomo, P.; Piraino, F. Vehicle-to-grid application with hydrogen-based tram. *Energy Convers. Manag.* **2021**, *250*, 114915. [CrossRef]

22. Blanco, H.; Faaij, A. A review at the role of storage in energy systems with a focus on Power to Gas and long-term storage. *Renew. Sustain. Energy Rev.* **2018**, *81*, 1049–1086. [CrossRef]

23. Juangsa, F.B.; Prananto, L.A.; Mufrodi, Z.; Budiman, A.; Oda, T.; Aziz, M. Highly energy-efficient combination of dehydrogenation of methylcyclohexane and hydrogen-based power generation. *Appl. Energy* **2018**, *226*, 31–38. [CrossRef]

24. Kovač, A.; Paranos, M.; Marciuš, D. Hydrogen in energy transition: A review. *Int. J. Hydrogen Energy* **2021**, *46*, 10016–10035. [CrossRef]

25. Arniella, V.; Zafra, A.; Álvarez, G.; Belzunce, J.; Rodríguez, C. Comparative study of embrittlement of quenched and tempered steels in hydrogen environments. *Int. J. Hydrogen Energy* **2022**, *47*, 17056–17068. [CrossRef]

26. Michler, T.; Naumann, J. Influence of high pressure hydrogen on the tensile and fatigue properties of a high strength Cu–Al–Ni–Fe alloy. *Int. J. Hydrogen Energy* **2010**, *35*, 11373–11377. [CrossRef]

27. Xu, Y.; Deng, Y.; Liu, W.; Zhao, X.; Xu, J.; Yuan, Z. Research progress of hydrogen energy and metal hydrogen storage materials. *Sustain. Energy Technol. Assess.* **2023**, *55*, 102974. [CrossRef]

28. Klopčič, N.; Grimmer, I.; Winkler, F.; Sartory, M.; Trattner, A. A review on metal hydride materials for hydrogen storage. *J. Energy Storage* **2023**, *72*, 108456. [CrossRef]

29. Chu, C.; Wu, K.; Luo, B.; Cao, Q.; Zhang, H. Hydrogen storage by liquid organic hydrogen carriers: Catalyst, renewable carrier, and technology—A review. *Carbon Resour. Convers.* **2023**, *6*, 334–351. [CrossRef]

30. Moradi, R.; Groth, K.M. Hydrogen storage and delivery: Review of the state of the art technologies and risk and reliability analysis. *Int. J. Hydrogen Energy* **2019**, *44*, 12254–12269. [CrossRef]

31. Lin, H.-J.; Lu, Y.-S.; Zhang, L.-T.; Liu, H.-Z.; Edalati, K.; Révész, Á. Recent advances in metastable alloys for hydrogen storage: A review. *Rare Met.* **2022**, *41*, 1797–1817. [CrossRef]

32. Wan, C.; Li, G.; Wang, J.; Xu, L.; Cheng, D.; Chen, F.; Asakura, Y.; Kang, Y.; Yamauchi, Y. Modulating Electronic Metal-Support Interactions to Boost Visible-Light-Driven Hydrolysis of Ammonia Borane: Nickel-Platinum Nanoparticles Supported on Phosphorus-Doped Titania. *Angew. Chem. Int. Ed.* **2023**, *62*, e202305371. [CrossRef]

33. Liu, J.; Yong, H.; Zhao, Y.; Wang, S.; Chen, Y.; Liu, B.; Hu, J.; Zhang, Y. Phase evolution, hydrogen storage thermodynamics, and kinetics of ternary $Mg_{98}Ho_{1.5}Fe_{0.5}$ alloy. *J. Rare Earths* 2023, *in press*. [CrossRef]

34. Wan, C.; Liang, Y.; Zhou, L.; Huang, J.; Wang, J.; Chen, F.; Zhan, X.; Cheng, D.-G. Integration of morphology and electronic structure modulation on cobalt phosphide nanosheets to boost photocatalytic hydrogen evolution from ammonia borane hydrolysis. *Green Energy Environ.* **2024**, *9*, 333–343. [CrossRef]

35. Abohamzeh, E.; Salehi, F.; Sheikholeslami, M.; Abbassi, R.; Khan, F. Review of hydrogen safety during storage, transmission, and applications processes. *J. Loss Prev. Process Ind.* **2021**, *72*, 104569. [CrossRef]

36. Barthelemy, H.; Weber, M.; Barbier, F. Hydrogen storage: Recent improvements and industrial perspectives. *Int. J. Hydrogen Energy* **2017**, *42*, 7254–7262. [CrossRef]
37. Gómez, J.A.; Santos, D.M.F. The Status of On-Board Hydrogen Storage in Fuel Cell Electric Vehicles. *Designs* **2023**, *7*, 97. [CrossRef]
38. Amaseder, F.; Krainz, G. Liquid Hydrogen Storage Systems Developed and Manufactured for the First Time for Customer Cars. In Proceedings of the SAE 2006 World Congress & Exhibition, Detroit, MI, USA, 3–6 April 2006. [CrossRef]
39. Aceves, S.M.; Espinosa-Loza, F.; Ledesma-Orozco, E.; Ross, T.O.; Weisberg, A.H.; Brunner, T.C.; Kircher, O. High-density automotive hydrogen storage with cryogenic capable pressure vessels. *Int. J. Hydrogen Energy* **2010**, *35*, 1219–1226. [CrossRef]
40. Nagumo, M. *Fundamentals of Hydrogen Embrittlement*; Springer: Singapore, 2016. [CrossRef]
41. Okonkwo, P.C.; Barhoumi, E.M.; Ben Belgacem, I.; Mansir, I.B.; Aliyu, M.; Emori, W.; Uzoma, P.C.; Beitelmal, W.H.; Akyüz, E.; Radwan, A.B.; et al. A focused review of the hydrogen storage tank embrittlement mechanism process. *Int. J. Hydrogen Energy* **2023**, *48*, 12935–12948. [CrossRef]
42. Siddiqui, R.A.; Abdullah, H.A. Hydrogen embrittlement in 0.31% carbon steel used for petrochemical applications. *J. Mater. Process Technol.* **2005**, *170*, 430–435. [CrossRef]
43. Capelle, J.; Gilgert, J.; Dmytrakh, I.; Pluvinage, G. Sensitivity of pipelines with steel API X52 to hydrogen embrittlement. *Int. J. Hydrogen Energy* **2008**, *33*, 7630–7641. [CrossRef]
44. Amaro, R.L.; Rustagi, N.; Findley, K.O.; Drexler, E.S.; Slifka, A.J. Modeling the fatigue crack growth of X100 pipeline steel in gaseous hydrogen. *Int. J. Fatigue* **2014**, *59*, 262–271. [CrossRef]
45. Nanninga, N.E.; Levy, Y.S.; Drexler, E.S.; Condon, R.T.; Stevenson, A.E.; Slifka, A.J. Comparison of hydrogen embrittlement in three pipeline steels in high pressure gaseous hydrogen environments. *Corros. Sci.* **2012**, *59*, 1–9. [CrossRef]
46. Gondal, I.A. Hydrogen transportation by pipelines. In *Compendium of Hydrogen Energy*; Elsevier: Amsterdam, The Netherlands, 2016; pp. 301–322. [CrossRef]
47. Genovese, M.; Pagnotta, L.; Piraino, F.; Fragiacomo, P. Fluid-dynamics analyses and economic investigation of offshore hydrogen transport via steel and composite pipelines. *Cell Rep. Phys. Sci.* **2024**, *5*, 101907. [CrossRef]
48. Tsiklios, C.; Hermesmann, M.; Müller, T.E. Hydrogen transport in large-scale transmission pipeline networks: Thermodynamic and environmental assessment of repurposed and new pipeline configurations. *Appl. Energy* **2022**, *327*, 120097. [CrossRef]
49. Mahajan, D.; Tan, K.; Venkatesh, T.; Kileti, P.; Clayton, C.R. Hydrogen Blending in Gas Pipeline Networks—A Review. *Energies* **2022**, *15*, 3582. [CrossRef]
50. Wang, H.; Tong, Z.; Zhou, G.; Zhang, C.; Zhou, H.; Wang, Y.; Zheng, W. Research and demonstration on hydrogen compatibility of pipelines: A review of current status and challenges. *Int. J. Hydrogen Energy* **2022**, *47*, 28585–28604. [CrossRef]
51. Dwivedi, S.K.; Vishwakarma, M. Hydrogen embrittlement in different materials: A review. *Int. J. Hydrogen Energy* **2018**, *43*, 21603–21616. [CrossRef]
52. Sharma, S.K.; Maheshwari, S. A review on welding of high strength oil and gas pipeline steels. *J. Nat. Gas. Sci. Eng.* **2017**, *38*, 203–217. [CrossRef]
53. Lei, Y.; Hosseini, E.; Liu, L.; Scholes, C.A.; Kentish, S.E. Internal polymeric coating materials for preventing pipeline hydrogen embrittlement and a theoretical model of hydrogen diffusion through coated steel. *Int. J. Hydrogen Energy* **2022**, *47*, 31409–31419. [CrossRef]
54. Li, P.; Chen, K.; Zhao, L.; Zhang, H.; Sun, H.; Yang, X.; Kim, N.H.; Lee, J.H.; Niu, Q.J. Preparation of modified graphene oxide/polyethyleneimine film with enhanced hydrogen barrier properties by reactive layer-by-layer self-assembly. *Compos. B Eng.* **2019**, *166*, 663–672. [CrossRef]
55. Barth, R.; Simmons, K.; San Marchi, C. *Polymers for Hydrogen Infrastructure and Vehicle Fuel Systems*; Sandia National Lab.: Albuquerque, NM, USA; Livermore, CA, USA, 2013. [CrossRef]
56. Stern, S.A.; Fried, J.R. *Permeability of Polymers to Gases and Vapors. Physical Properties of Polymers Handbook*; Springer: New York, NY, USA, 2007; pp. 1033–1047. [CrossRef]
57. Klopffer, M.H.; Flaconneche, B. Transport Properdines of Gases in Polymers: Bibliographic Review. *Oil Gas. Sci. Technol.* **2001**, *56*, 223–244. [CrossRef]
58. Flaconneche, B.; Martin, J.; Klopffer, M.H. Transport Properties of Gases in Polymers: Experimental Methods. *Oil Gas Sci. Technol.* **2001**, *56*, 245–259. [CrossRef]
59. Michaels, A.S.; Bixler, H.J. Flow of gases through polyethylene. *J. Polym. Sci.* **1961**, *50*, 413–439. [CrossRef]
60. Prasad, K.; Nikzad, M.; Sbarski, I. Permeability control in polymeric systems: A review. *J. Polym. Res.* **2018**, *25*, 232. [CrossRef]
61. *UNI EN ISO 11114-5:2022*; Bombole per Gas—Compatibilità dei Materiali della Bombola e della Valvola con i Gas Contenuti—Parte 5: Metodi di Prova per la Valutazione dei Rivestimenti di Plastica. ISO: Geneva, Switzerland, 2022.
62. *ISO 19881:2018*; Gaseous Hydrogen—Land Vehicle Fuel Containers. ISO: Geneva, Switzerland, 2018.
63. Maus, S.; Hapke, J.; Ranong, C.N.; Wüchner, E.; Friedlmeier, G.; Wenger, D. Filling procedure for vehicles with compressed hydrogen tanks. *Int. J. Hydrogen Energy* **2008**, *33*, 4612–4621. [CrossRef]
64. Li, X.; Huang, Q.; Liu, Y.; Zhao, B.; Li, J. Review of the Hydrogen Permeation Test of the Polymer Liner Material of Type IV On-Board Hydrogen Storage Cylinders. *Materials* **2023**, *16*, 5366. [CrossRef]
65. Sun, Y.; Lv, H.; Zhou, W.; Zhang, C. Research on hydrogen permeability of polyamide 6 as the liner material for type IV hydrogen storage tank. *Int. J. Hydrogen Energy* **2020**, *45*, 24980–24990. [CrossRef]
66. Van Amerongen, G.J. Influence of structure of elastomers on their permeability to gases. *J. Polym. Sci.* **1950**, *5*, 307–332. [CrossRef]

67. Van Amerongen, G.J. The Permeability of Different Rubbers to Gases and Its Relation to Diffusivity and Solubility. *J. Appl. Phys.* **1946**, *17*, 972–985. [CrossRef]
68. Humpenöder, J. Gas permeation of fibre reinforced plastics. *Cryogenics* **1998**, *38*, 143–147. [CrossRef]
69. Tikhomirov, B.P.; Hopfenberg, H.B.; Stannett, V.; Williams, J.L. Permeation, diffusion, and solution of gases and water vapor in unplasticized poly(vinylchloride). *Die Makromol. Chem.* **1968**, *118*, 177–188. [CrossRef]
70. Rogers, C.E. Permeation of Gases and Vapours in Polymers. In *Polymer Permeability*; Springer: Dordrecht, The Netherlands, 1985; pp. 11–73. [CrossRef]
71. Oseli, A.; Aulova, A.; Gergesova, M.; Emri, I. Effect of Temperature on Mechanical Properties of Polymers. In *Encyclopedia of Continuum Mechanics*; Springer: Berlin/Heidelberg, Germany, 2019; pp. 1–20. [CrossRef]
72. Fujiwara, H.; Ono, H.; Onoue, K.; Nishimura, S. High-pressure gaseous hydrogen permeation test method -property of polymeric materials for high-pressure hydrogen devices (1)-. *Int. J. Hydrogen Energy* **2020**, *45*, 29082–29094. [CrossRef]
73. Naito, Y.; Bourbon, D.; Terada, K.; Kamiya, Y. Permeation of high-pressure gases in poly(ethylene-*co*-vinyl acetate). *J. Polym. Sci. B Polym. Phys.* **1993**, *31*, 693–697. [CrossRef]
74. Stern, S.A.; Fang, S.-M.; Frisch, H.L. Effect of pressure on gas permeability coefficients. A new application of "free volume" theory. *J. Polym. Sci. Part A-2 Polym. Phys.* **1972**, *10*, 201–219. [CrossRef]
75. Fumitoshi, K.; Hirotada, F.; Shin, N. Influence of high-pressure hydrogen gas on crystalline polymers. In Proceedings of the 33rd Polymer Degradation Discussion Group, St. Julians, Malta, 1–5 September 2019.
76. Castagnet, S.; Grandidier, J.-C.; Comyn, M.; Benoît, G. Hydrogen influence on the tensile properties of mono and multi-layer polymers for gas distribution. *Int. J. Hydrogen Energy* **2010**, *35*, 7633–7640. [CrossRef]
77. Stelitano, S.; Rullo, A.; Piredda, L.; Mecozzi, E.; Di Vito, L.; Agostino, R.G.; Filosa, R.; Formoso, V.; Conte, G.; Policicchio, A. The Deltah Lab, a New Multidisciplinary European Facility to Support the H_2 Distribution & Storage Economy. *Appl. Sci.* **2021**, *11*, 3272. [CrossRef]
78. Castagnet, S.; Grandidier, J.-C.; Comyn, M.; Benoît, G. Effect of long-term hydrogen exposure on the mechanical properties of polymers used for pipes and tested in pressurized hydrogen. *Int. J. Press. Vessel. Pip.* **2012**, *89*, 203–209. [CrossRef]
79. Castagnet, S.; Grandidier, J.-C.; Comyn, M.; Benoît, G. Mechanical Testing of Polymers in Pressurized Hydrogen: Tension, Creep and Ductile Fracture. *Exp. Mech.* **2012**, *52*, 229–239. [CrossRef]
80. Alvine, K.J.; Kafentzis, T.A.; Pitman, S.G.; Johnson, K.I.; Skorski, D.; Tucker, J.C.; Roosendaal, T.J.; Dahl, M.E. An in situ tensile test apparatus for polymers in high pressure hydrogen. *Rev. Sci. Instrum.* **2014**, *85*, 105110. [CrossRef]
81. Yamabe, J.; Nishimura, S. Influence of carbon black on decompression failure and hydrogen permeation properties of filled ethylene-propylene–diene–methylene rubbers exposed to high-pressure hydrogen gas. *J. Appl. Polym. Sci.* **2011**, *122*, 3172–3187. [CrossRef]
82. Yamabe, J.; Nishimura, S. Influence of fillers on hydrogen penetration properties and blister fracture of rubber composites for O-ring exposed to high-pressure hydrogen gas. *Int. J. Hydrogen Energy* **2009**, *34*, 1977–1989. [CrossRef]
83. Menon, N.C.; Kruizenga, A.M.; Alvine, K.J.; San Marchi, C.; Nissen, A.; Brooks, K. *Behaviour of Polymers in High Pressure Environments as Applicable to the Hydrogen Infrastructure*; Volume 6B: Materials and Fabrication; American Society of Mechanical Engineers: New York, NY, USA, 2016. [CrossRef]
84. Theiler, G.; Cano Murillo, N.; Halder, K.; Balasooriya, W.; Hausberger, A.; Kaiser, A. Effect of high-pressure hydrogen environment on the physical and mechanical properties of elastomers. *Int. J. Hydrogen Energy* **2024**, *58*, 389–399. [CrossRef]
85. Michaels, A.S.; Parker, R.B. Sorption and flow of gases in polyethylene. *J. Polym. Sci.* **1959**, *41*, 53–71. [CrossRef]
86. Michaels, A.S.; Bixler, H.J. Solubility of gases in polyethylene. *J. Polym. Sci.* **1961**, *50*, 393–412. [CrossRef]
87. Nishimura, S. Fracture Behavior of Ethylene Propylene Rubber for Hydrogen Gas Sealing Under High-pressure Hydrogen. *Nippon Gomu Kyokaishi* **2013**, *86*, 360–366. [CrossRef]
88. Potts, J.R.; Dreyer, D.R.; Bielawski, C.W.; Ruoff, R.S. Graphene-based polymer nanocomposites. *Polymer* **2011**, *52*, 5–25. [CrossRef]
89. Choudalakis, G.; Gotsis, A.D. Permeability of polymer/clay nanocomposites: A review. *Eur. Polym. J.* **2009**, *45*, 967–984. [CrossRef]
90. Gatos, K.G.; Karger-Kocsis, J. Effect of the aspect ratio of silicate platelets on the mechanical and barrier properties of hydrogenated acrylonitrile butadiene rubber (HNBR)/layered silicate nanocomposites. *Eur. Polym. J.* **2007**, *43*, 1097–1104. [CrossRef]
91. Takeyama, Y.; Ueno, M.; Uejima, M.; Fujiwara, H.; Nishimura, S. Development of Carbon Nanotube/Rubber Composite Materials with Excellent High Pressure Hydrogen Characteristics. *Kobunshi Ronbunshu* **2019**, *76*, 288–296. [CrossRef]
92. Briscoe, B.J.; Savvas, T.; Kelly, C.T. "Explosive Decompression Failure" of Rubbers: A Review of the Origins of Pneumatic Stress Induced Rupture in Elastomers. *Rubber Chem. Technol.* **1994**, *67*, 384–416. [CrossRef]
93. Lorge, O.; Briscoe, B.J.; Dang, P. Gas induced damage in poly(vinylidene fluoride) exposed to decompression. *Polymer* **1999**, *40*, 2981–2991. [CrossRef]
94. Yamabe, J.; Nishimura, S. Nanoscale fracture analysis by atomic force microscopy of EPDM rubber due to high-pressure hydrogen decompression. *J. Mater. Sci.* **2011**, *46*, 2300–2307. [CrossRef]
95. Yamabe, J.; Matsumoto, T.; Nishimura, S. Application of acoustic emission method to detection of internal fracture of sealing rubber material by high-pressure hydrogen decompression. *Polym. Test.* **2011**, *30*, 76–85. [CrossRef]
96. Jaravel, J.; Castagnet, S.; Grandidier, J.-C.; Gueguen, M. Experimental real-time tracking and diffusion/mechanics numerical simulation of cavitation in gas-saturated elastomers. *Int. J. Solids Struct.* **2013**, *50*, 1314–1324. [CrossRef]

97. Jaravel, J.; Castagnet, S.; Grandidier, J.-C.; Benoît, G. On key parameters influencing cavitation damage upon fast decompression in a hydrogen saturated elastomer. *Polym. Test.* **2011**, *30*, 811–818. [CrossRef]
98. Kane-Diallo, O.; Castagnet, S.; Nait-Ali, A.; Benoit, G.; Grandidier, J.-C. Time-resolved statistics of cavity fields nucleated in a gas-exposed rubber under variable decompression conditions—Support to a relevant modeling framework. *Polym. Test.* **2016**, *51*, 122–130. [CrossRef]
99. Yersak, T.A.; Baker, D.R.; Yanagisawa, Y.; Slavik, S.; Immel, R.; Mack-Gardner, A.; Herrmann, M.; Cai, M. Predictive model for depressurization-induced blistering of type IV tank liners for hydrogen storage. *Int. J. Hydrogen Energy* **2017**, *42*, 28910–28917. [CrossRef]
100. Baldwin, D. *Final Report—Development of High Pressure Hydrogen Storage Tank for Storage and Gaseous Truck Delivery*; Hexagon Lincoln LLC: Golden, CO, USA, 2017. [CrossRef]
101. Melnichuk, M.; Thiébaud, F.; Perreux, D. Non-dimensional assessments to estimate decompression failure in polymers for hydrogen systems. *Int. J. Hydrogen Energy* **2020**, *45*, 6738–6744. [CrossRef]
102. Ono, H.; Fujiwara, H.; Onoue, K.; Nishimura, S. Influence of repetitions of the high-pressure hydrogen gas exposure on the internal damage quantity of high-density polyethylene evaluated by transmitted light digital image. *Int. J. Hydrogen Energy* **2019**, *44*, 23303–23319. [CrossRef]
103. El-Sawy, K.M. Inelastic stability of tightly fitted cylindrical liners subjected to external uniform pressure. *Thin-Walled Struct.* **2001**, *39*, 731–744. [CrossRef]
104. Rueda, F.; Otegui, J.L.; Frontini, P. Numerical tool to model collapse of polymeric liners in pipelines. *Eng. Fail. Anal.* **2012**, *20*, 25–34. [CrossRef]
105. Pepin, J.; Lainé, E.; Grandidier, J.-C.; Castagnet, S.; Blanc-Vannet, P.; Papin, P.; Weber, M. Determination of key parameters responsible for polymeric liner collapse in hyperbaric type IV hydrogen storage vessels. *Int. J. Hydrogen Energy* **2018**, *43*, 16386–16399. [CrossRef]
106. Pépin, J.; Lainé, E.; Grandidier, J.-C.; Benoit, G.; Mellier, D.; Weber, M.; Langlois, C. Replication of liner collapse phenomenon observed in hyperbaric type IV hydrogen storage vessel by explosive decompression experiments. *Int. J. Hydrogen Energy* **2018**, *43*, 4671–4680. [CrossRef]
107. Mandal, S.; Dasmahapatra, A.K. Effect of aging on the microstructure and physical properties of Poly(vinyl alcohol) hydrogel. *J. Polym. Res.* **2021**, *28*, 269. [CrossRef]
108. Balasooriya, W.; Clute, C.; Schrittesser, B.; Pinter, G. A Review on Applicability, Limitations, and Improvements of Polymeric Materials in High-Pressure Hydrogen Gas Atmospheres. *Polym. Rev.* **2022**, *62*, 175–209. [CrossRef]
109. Kim, M.; Lee, C.H. Hydrogenation of High-Density Polyethylene during Decompression of Pressurized Hydrogen at 90 MPa: A Molecular Perspective. *Polymers* **2023**, *15*, 2880. [CrossRef]
110. Yamabe, J.; Fujiwara, H.; Nishimura, S. Fracture Analysis of Rubber Sealing Material for High Pressure Hydrogen Vessel. *J. Environ. Eng.* **2011**, *6*, 53–68. [CrossRef]
111. Fujiwara, H.; Ono, H.; Nishimura, S. Degradation behavior of acrylonitrile butadiene rubber after cyclic high-pressure hydrogen exposure. *Int. J. Hydrogen Energy* **2015**, *40*, 2025–2034. [CrossRef]